

Impact of episodic vertical fluxes on sea surface pCO₂

BY A. MAHADEVAN¹, A. TAGLIABUE², L. BOPP², A. LENTON³, L. MÉMERY⁴,
M. LÉVY⁵

1. *Department of Earth Sciences, Boston University, Boston, MA, USA*

2. *LSCE-IPSL, CNRS/CEA/UVSQ, Gif-sur-Yvette, France*

3. *CSIRO Wealth from Oceans National Research Flagship, Hobart, TAS, Australia*

4. *LEMAR, UBO/CNRS/IRD, Plouzane, France*

5. *LOCEAN-IPSL, CNRS/UPMC/IRD/MNHN, Paris, France*

Corresponding Author: marina.levy@upmc.fr

15 February 2010

Revised 20 September 2010

ABSTRACT

Episodic events like hurricanes, storms, and frontal- and eddy-driven upwelling can alter the partial pressure of CO₂ at the sea surface (pCO₂) by entraining subsurface waters into the surface mixed layer of the ocean. Since pCO₂ is a function of total dissolved inorganic carbon (DIC), temperature (T), salinity (S) and alkalinity (ALK), it responds to the combined impacts of physical, chemical, and biological changes. Here we present an analytical framework for assessing the relative magnitude and sign in the short term perturbation of surface pCO₂ arising from vertical mixing events. Using global, monthly, climatological datasets, we assess the individual, as well as integrated, contribution of various properties to surface pCO₂ in response to episodic mixing. The response depends on the relative vertical gradients of properties beneath the mixed layer. Many areas of the ocean exhibit very little sensitivity to mixing due to the compensatory effects of DIC and T on pCO₂, whereas others, such as the eastern upwelling margins, have the potential to generate large positive/negative anomalies in surface pCO₂. The response varies seasonally and spatially and becomes more intense in subtropical and subpolar regions during summer. Regions showing a greater pCO₂ response to vertical mixing are likely to exhibit higher spatial variability in surface pCO₂ on time scales of days.

Keywords: CO₂, oceanic pCO₂, DIC, sea surface variability, vertical mixing

1. Introduction

The ocean plays a critical role in mitigating climate change taking up nearly 30% of anthropogenic CO₂ emissions, (Le Quéré *et al.*, 2009). The air-sea flux of CO₂ depends on the difference in the partial pressures of CO₂ (pCO₂) between the atmosphere and sea surface, as well as wind speed and air-sea interfacial conditions,

[e.g. Wanninkhof (1992)]. Oceanic surface pCO₂ is a function of dissolved inorganic carbon (DIC), temperature (T), salinity (S) and alkalinity (ALK). Hence, it responds to physical processes such as mixing, deep convection, and water mass transformation, as well as biological processes like net primary production (NPP) and remineralization of organic matter. Each of the drivers of oceanic pCO₂ has its own temporal and spatial scales of response to dynamical change. Unsurprisingly, surface pCO₂ is highly variable in space and time, and much of the variability occurs on short timescales (Lenton *et al.*, 2006). Global studies have focussed on understanding the large-scale, seasonal patterns in sea surface pCO₂ and in quantifying the related air-sea fluxes of CO₂ at coarse spatial and temporal resolution ($4^{\circ} \times 5^{\circ}$ monthly; Takahashi, *et al.* (2009)). On the other hand, disparate findings have been reported about the variability and controlling factors of surface pCO₂ on short space and time scales (Archer *et al.*, 1996; DeGrandpre *et al.*, 1997; Borges & Frankignoulle, 2001; Copin-Montégut *et al.*, 2004; Körtzinger *et al.*, 2008; Leinweber *et al.*, 2009; Merlivat *et al.*, 2009), suggesting that there is clearly need for a unified, mechanistic understanding of how surface pCO₂ responds to episodic, localized events that induce vertical mixing.

While the surface layer of the ocean is fairly well mixed, there are strong gradients in the vertical distribution of properties beneath the mixed layer (ML). With increasing depth, T decreases, DIC, S and nutrients increase, whereas ALK can increase or decrease depending on depth and location. Therefore any physical process that generates localized overturning, up-/down-welling or diapycnal mixing, and entrains water from below the ML, can change the physical-chemical properties in the surface mixed layer. This, along with any subsequent biological changes in response to it, can significantly perturb the mean state of surface pCO₂. We will refer to processes that lead to a vertical flux of properties across the base of the ML, more generally, as “mixing”. Potential mechanisms that can induce such events include negative buoyancy fluxes causing convection, frontal dynamics (Pollard & Regier, 1992; Klein *et al.*, 2008), localized upwelling/mixing due to wind variability (Hales *et al.*, 2005), storms and hurricanes (Bates *et al.*, 1998), and proposed geo-engineering schemes such as ocean pipes (Lovelock & Rapley, 2007). Indeed the importance of such vertical mixing events on phytoplankton production and the biological pump are now widely recognized (Klein & Coste, 1984; McGillicuddy, Jr. *et al.*, 1998; Mahadevan & Archer, 2000; Lévy *et al.*, 2001, 2009). However, their effect on surface pCO₂ is more complex and difficult to generalize due to the multiple factors that control pCO₂.

Several regional studies have examined the short-term response of sea surface pCO₂ to mixing events. Modeling studies of the eastern North Atlantic found little or no change in the surface pCO₂ in response to upwelling induced by fronts and eddies because additional DIC was counter-balanced by reduced temperature (Mahadevan *et al.*, 2004; Resplandy *et al.*, 2009). Perrie *et al.* (2004) and Bates *et al.* (1998) reported opposing changes in surface pCO₂ in response to hurricane events. These studies highlight the complex interactions of the drivers of oceanic pCO₂ and the difficulty in generalizing the response globally. While global modeling studies (Dutreuil *et al.*, 2009; Yool *et al.*, 2009) that evaluated the ocean pipe geo-engineering schemes examine biological and physical changes due to vertical fluxes, these studies focused on the longer-term impacts through the implementation of a quasi-permanent perturbation to the system. Nevertheless, they also highlight the

high degree of spatial variability in the biological and physical response to vertical fluxes.

In this study we develop a general theoretical framework, accounting for physical and biological changes in response to mixing, such that the modulation of surface $p\text{CO}_2$ by individual properties, as well as their integrated effect, can be understood on short time scales. The magnitude of the response depends not only on the intensity and duration of the mixing, but also on the location and timing of the events. We quantify the response of surface $p\text{CO}_2$ in terms of the contributions from changes in DIC, T, S and ALK. The sum of these changes can act to either increase or decrease $p\text{CO}_2$. We evaluate these contributions and their integral effect using climatological observations of T, DIC, ALK, nitrate (NO_3) and S. In this study, we apply our framework for assessing short term perturbations from the monthly, mean, climatological distributions. It is complementary to studies of climatological, monthly $p\text{CO}_2$ variability that include the large-scale longer-term response but ignore the short spatial and temporal scale response. It provides a context and mechanistic framework in which differing regional responses can be interpreted. But, the method may also be used with other observational data to examine perturbations arising from specific events on a regional scale.

The theoretical framework we present here addresses time scales representative of events lasting up to a few days. We neglect the air-sea exchange of heat, freshwater, and CO_2 in our calculations. Horizontal transport is neglected and only vertical fluxes due to various processes (advective and diapycnal) are represented through a vertical eddy diffusivity acting at the base of the mixed layer. For the sake of this analysis, the MLD and vertical profiles of the oceanic properties (T, DIC, ALK, NO_3) are assumed not to be modified by the vertical mixing. Redfield ratios are used to estimate biological uptake of DIC and only NO_3 is considered as a limiting nutrient (e.g. iron or silicate limitation is neglected). Our analysis relies on using modern (World Ocean Atlas, 2005) climatologies of temperature (Locarnini *et al.*, 2006), salinity (Antonov *et al.*, 2006), and NO_3 (Garcia *et al.*, 2006), DIC, and ALK (Key *et al.*, 2004, GLODAP). We realize that these data sets are based on sparse measurements; they may not be reliable in some regions such as the Southern ocean and do not resolve the seasonal variability in DIC and ALK. Our approach is to apply the proposed framework to the best available global data sets in the hope that the broad conclusions are qualitatively correct and will be tested with better data sets in the future. In applying the approach to these data sets, we assume that these large scale properties are not changing with time, apart from changes due to the seasonal cycle that are explicitly or implicitly taken into account in our study. Thus our results only apply for the modern state and ignore inter-annual/decadal variability of ocean properties as well as any long-term trends in those properties. Any long-term changes in mixing or property sources/sinks would alter mean distributions and also bring into effect air-sea fluxes and horizontal circulation. Thus our analysis applies to episodic mixing.

2. Theoretical framework

To quantify the effect of localized upwelling or vertical mixing on surface $p\text{CO}_2$, we express the rate of change of $p\text{CO}_2$ in terms of the various properties on which it

119 is dependent (Takahashi *et al.*, 1993) as follows

$$120 \quad \frac{\partial \text{pCO}_2}{\partial t} = \frac{\partial \text{pCO}_2}{\partial T} \frac{\partial T}{\partial t} + \frac{\partial \text{pCO}_2}{\partial \text{DIC}} \frac{\partial \text{DIC}}{\partial t} + \frac{\partial \text{pCO}_2}{\partial \text{ALK}} \frac{\partial \text{ALK}}{\partial t} + \frac{\partial \text{pCO}_2}{\partial S} \frac{\partial S}{\partial t}. \quad (2.1)$$

121 In order to consider the response of the surface mixed layer to small-scale upwelling
 122 and/or mixing, we model the vertical flux of any property χ , as a diffusive flux
 123 described by $\kappa \frac{\partial \chi}{\partial z}$, where κ denotes the vertical eddy diffusivity of the property.
 124 This is meant to account for mixing, as well as localized vertical advective fluxes
 125 that occur at horizontal scales much smaller than the resolution of our datasets
 126 (nominally $1^0 \times 1^0$). We therefore assume the value of κ to be the same for all the
 127 properties. The rate of change in any property χ within the ML of depth H , is
 128 modeled as

$$129 \quad \frac{\partial \chi}{\partial t} = -\frac{1}{H} \kappa \frac{\partial \chi}{\partial z} \Big|_{z=-H} + S_\chi. \quad (2.2)$$

130 Here, we consider only a one-dimensional budget for χ to evaluate the effects of
 131 vertical mixing/upwelling. The property χ is assumed to be uniformly mixed within
 132 the ML and any sources/sinks that alter the property in the ML (other than air-sea
 133 fluxes) are denoted by S_χ . Further, $\frac{\partial \chi}{\partial z} \Big|_{z=-H}$ is the vertical gradient across the base
 134 of the mixed layer ($z = -H$) that results in a vertical flux into the ML.

135 We note that the Revelle factors for DIC and ALK, namely,

$$136 \quad \xi = \frac{\Delta \text{pCO}_2}{\text{pCO}_2} / \frac{\Delta \text{DIC}}{\text{DIC}} \Big|_{\text{ALK}=\text{const}} \quad \xi_A = \frac{\Delta \text{pCO}_2}{\text{pCO}_2} / \frac{\Delta \text{ALK}}{\text{ALK}} \Big|_{\text{DIC}=\text{const}} \quad (2.3)$$

137 are variable in space and time with typical values in the range 8–15 for ξ , and -8 –
 138 -13 for ξ_A (Sarmiento & Gruber, 2006). For the salinity and temperature range of
 139 the ocean, there is a well established relationship between pCO_2 and T , as well as
 140 S , (Takahashi *et al.*, 1993)

$$141 \quad \beta = \frac{1}{\text{pCO}_2} \frac{\partial \text{pCO}_2}{\partial T} = 0.0423 \text{ } ^\circ\text{C}^{-1}, \quad \beta_s = \frac{1}{\text{pCO}_2} \frac{\partial \text{pCO}_2}{\partial S} = 0.9^{-1}. \quad (2.4)$$

142 To evaluate the relative change in surface pCO_2 in response to vertical fluxes, we
 143 divide both sides of (2.1) by the value of pCO_2 in the surface layer. Using (2.2)
 144 along with the relationships (2.3) and (2.4), and expressing the time rate of change
 145 of pCO_2 as $\frac{\Delta \text{pCO}_2}{\Delta t}$ we can rewrite (2.1) as

$$146 \quad \frac{\Delta \text{pCO}_2}{\text{pCO}_2} = -\frac{\kappa \Delta t}{H} \left(\beta \frac{\partial T}{\partial z} + \frac{\xi}{\text{DIC}} \frac{\partial \text{DIC}}{\partial z} + \frac{\xi_A}{\text{ALK}} \frac{\partial \text{ALK}}{\partial z} + \beta_S \frac{\partial S}{\partial z} \right) \\ 147 \quad + S_T + S_{\text{DIC}} + S_{\text{ALK}} + S_S. \quad (2.5)$$

148 This equation describes the relative change in surface pCO_2 arising from the in-
 149 dividual responses of DIC, ALK, T and S to vertical mixing across the base of
 150 the mixed layer. All values, other than the gradients, are determined in the mixed
 151 layer. The first four parenthesized terms on the right hand side of (2.5) denote
 152 the relative change in pCO_2 due to the vertical mixing of T , DIC, ALK and S ,
 153 whereas the next four terms denote the relative pCO_2 change due to sources and
 154 sinks for T , DIC, ALK and S . We consider perturbations to the surface pCO_2 due
 155 to vertical oceanic transport alone, while neglecting the atmospheric response, i.e.

air-sea fluxes in response to the altered surface pCO₂. In other words, we consider the perturbation in surface pCO₂ due to episodic oceanic processes, but not the consequent air-sea equilibration that is expected to occur on longer time scales (weeks to months) toward neutralizing such perturbations. Surface fluxes of heat, freshwater and CO₂ are therefore not included. Thus, $S_T = S_S = 0$ and S_{DIC} and S_{ALK} account for biological effects. More precisely, S_{DIC} accounts for the uptake of DIC by biological consumption. Vertical mixing and advection supplies remineralized nutrients to the surface ocean and stimulates NPP. Since NPP is limited by NO₃ in much of the ocean, we calculate the maximum potential consumption of DIC during NPP by multiplying the NO₃ supplied through vertical mixing with the Redfield C/N ratio, $R_{C:N} = 6.625$. To account for light limitation associated with deepened mixed layers, we multiply the potential DIC consumption by a light limitation factor $L = 1 - \exp(-(E/E_k))$ that varies between 0 and 1 depending on the mean light availability over the mixed layer. Here E is the climatological mixed layer average of photosynthetically available radiation (PAR) and E_k is a light limitation constant taken to be 80 μ -Einsteins m⁻²s⁻¹. The relative change in pCO₂ due to the biological consumption of DIC is thus modeled as

$$S_{DIC} = -\frac{\kappa \Delta t}{H} \left(\frac{\xi}{DIC} R_{C:N} L \frac{\partial \text{NO}_3}{\partial z} \right). \quad (2.6)$$

The NO₃ that is supplied by mixing, but is left unconsumed by NPP due to light limitation, contributes alkalinity, which results in a relative change in pCO₂ calculated as

$$S_{ALK} = \frac{\kappa \Delta t}{H} \left(\frac{\xi_A}{ALK} \frac{\partial \text{NO}_3}{\partial z} (1 - L) \right). \quad (2.7)$$

For much of the ocean, it is reasonable to assume that NO₃ limits biological production. However, in the high nutrient low chlorophyll (HNLC) regions of the world's ocean (primarily the Southern, sub-Arctic Pacific and Equatorial Pacific Oceans), the micronutrient iron (Fe) limits biological productivity. Taking into account the limitation of Fe or other potentially limiting nutrients like phosphate or silicic acid requires knowledge of that nutrient's distribution and the nutrient-specific limitation in phytoplankton production at each location, which we lack and thus do not include. Similarly, potential changes in species composition and alkalinity consumption during calcification or bacterial remineralization are not accounted for in this study.

3. Datasets and Methods

We use a number of different global climatological data sets to evaluate the various terms in (2.5), which define the contribution of mixing of individual properties on the relative change in surface pCO₂. Mixed layer depth (MLD), H , based on the fixed density criterion of 0.03 kg-m⁻³ is taken from the monthly climatology of de Boyer Montégut *et al.* (2004). To facilitate a common analysis we interpolate all the data on to the 1° × 1° grid used in the GLObal Ocean Data Analysis Project (Key *et al.*, 2004, GLODAP). The GLODAP database (Key *et al.*, 2004) provides an annual mean distribution of DIC and ALK mapped on a 1° × 1° grid globally, though it should be remembered that the average spacing between the cruises that

make up the GLODAP data often exceeds 10^0 . To account for the seasonality in surface DIC and ALK arising from mixed layer variations, we average the GLODAP values within the mixed layer, whose depth varies from month to month. This gives us a monthly, mixed layer DIC and ALK distribution, which includes seasonality in the MLD, but does not include effects arising from seasonality in biological production and consumption. Such an approach is justified because the removal of DIC by biology contributes only a very small perturbation to the total DIC and its mean profile. Furthermore, a comparison between these monthly DIC and ALK fields estimated for the ML, and monthly surface DIC and ALK computed from the surface $p\text{CO}_2$ climatology (Takahashi, et al., 2009) using an empirical computation of salinity and carbon chemistry (Lenton *et al.*, submitted), reveals that the differences are insignificant for the purposes of this study.

We use monthly values of PAR from the SeaWiFS climatology calculated over the period 199(7-8) to 2009 (<http://oceancolor.gsfc.nasa.gov/cgi/l3>). This $8\text{km} \times 8\text{km}$ resolution monthly data is averaged onto the $1^0 \times 1^0$ grid used in this study. To account for the small biological response of the austral and boreal winters, we set the missing values to be $1.25 \text{ Einsteins m}^{-2} \text{ day}^{-1}$. We include the effect of albedo on PAR by using the monthly mean fractional sea ice cover and assuming that when sea ice cover exceeds 50%, PAR is reduced by a factor of 0.5. Our value of 0.5 accounts for the combined albedos of open ocean (0.1), sea ice (0.5–0.7) and snow covered sea ice (0.8–0.9). Climatological values of sea ice are from Walsh (1978) and Zwally *et al.* (1983). We estimate an average value of PAR for the ML using Beer’s law for Type 1 waters (Lengaigne *et al.*, 2009) with an e-folding depth scale of 23m for the attenuation of light downward from the surface.

Monthly temperature (Locarnini *et al.*, 2006), salinity (Antonov *et al.*, 2006), and NO_3 (Garcia *et al.*, 2006) are obtained from the World Ocean Atlas (WOA05) and regridded on to the GLODAP grid. We average these fields within the mixed layer for each month to obtain a uniform mixed layer value that we use for consistency with the DIC and ALK fields.

To convert the change in DIC and ALK to $p\text{CO}_2$ we use the approximate empirical relationships for Revelle factors of ALK and DIC following Sarmiento & Gruber (2006); $\xi = \frac{3 \cdot \text{ALK} \cdot \text{DIC} - 2 \cdot \text{DIC}^2}{(2 \cdot \text{DIC} - \text{ALK}) \cdot (\text{ALK} - \text{DIC})}$; $\xi_A = \frac{\text{ALK}^2}{(2 \cdot \text{DIC} - \text{ALK})(\text{ALK} - \text{DIC})}$. We calculate these values monthly to account for seasonal changes in surface DIC and ALK.

The vertical gradients of properties at the base of the mixed layer are derived by differencing the ML value of the property (described as obtained above) with the value just beneath the mixed layer on the GLODAP grid. Since MLD varies from month to month, so do the gradients at the base of the MLD. The evaluation of vertical gradients in this manner neglects perturbations to the MLD arising from the localized mixing/upwelling events.

In order to compare the relative effects of T, DIC, ALK and the biological uptake of DIC for a given strength of vertical mixing or upwelling (characterized by κ) occurring over a time scale representative of synoptic events, we choose $\kappa = 10^{-3} \text{m}^2 \text{s}^{-1}$ and $\Delta t = 1 \text{ day}$ in evaluating each of the terms in equation (2.5). Here κ represents the vertical eddy diffusivity at the base of the mixed layer arising from mixing (e.g. due to upwelling, wind- or convection-induced overturning or entrainment), and Δt represents the duration of the episodic mixing event. The

specific values of κ would depend on the intensity of the mixing event, strength of stratification and vertical shear at the base of the mixed layer. We do not expect κ to be uniform in time and space, but by choosing a constant value, we are assessing the response of surface $p\text{CO}_2$ to the same intensity of mixing or upwelling applied at any location. The value of Δt is representative of the duration of an episodic mixing event. A larger (or smaller) value of κ or Δt would simply result in an equivalently larger (or smaller) response that can be linearly scaled from the results presented.

The relative $p\text{CO}_2$ change due to mixing is estimated globally using the monthly climatological data sets as the sum of various contributions. The physical effects of vertically mixing T, DIC, ALK, S, are cumulatively termed the “abiotic” response, in contrast to the biological response arising from the consumption of DIC in Redfield proportion to the vertically fluxed NO_3 . The increase in alkalinity arising from any excess (unconsumed) NO_3 is also included in the biological response, but is negligible. The effect of salinity perturbations on $p\text{CO}_2$ is negligible compared to the other factors and is not discussed further or presented separately.

Before presenting our results, we assess their sensitivity to variations in the MLD. Recomputing the effect of mixing on the relative change in surface $p\text{CO}_2$ with the climatological MLD altered by $\pm 20\%$ reveals very little sensitivity to a relative change in MLD. MLD variations are significant only when the ML is shallow ($< 50\text{m}$ in summer). At such times, a large relative perturbation to MLD (which could be small in absolute terms) is required to produce a change in the response.

4. Results

(a) Varied response of surface $p\text{CO}_2$ to mixing

The net response of surface $p\text{CO}_2$ to vertical mixing is highly variable in space and time. Figs. 1a,b are global maps of the relative change in surface $p\text{CO}_2$ arising from mixing during January and July. Mixing of the same intensity ($\kappa = 10^{-3}\text{m}^2\text{s}^{-1}$) and duration ($\Delta t = 1$ day) is applied globally at the base of the ML to make this assessment. Warm colours (yellow and reds) indicate regions where vertical mixing would enhance the surface $p\text{CO}_2$, whereas cool colours indicate where $p\text{CO}_2$ would be lowered. Large areas of the ocean (coloured in grey or in light shades) show little sensitivity to vertical mixing. While some regions indicate an increase in $p\text{CO}_2$ due to vertical fluxes, others would experience a decrease. Sensitivity to vertical mixing becomes enhanced in stratified regions; hence a much larger response is seen in the hemisphere experiencing summer. This single factor of summertime stratification gives rise to a large seasonality in the response of surface $p\text{CO}_2$. A large response is also found on the eastern upwelling margins of the ocean basins. Though we use a colour bar between $\pm 5\%$, the maximum range (for the chosen value of mixing) extends from -27% to $+36\%$. This range, extending from negative to positive, indicates that the same mixing event acting in different locations could elicit a completely opposite response. In some regions, contrasting or opposite tendencies are seen to occur in close proximity of one another. For example, on either side of the Kuroshio and Gulf Stream, and along the eastern equatorial margins, we see alternating positive and negative responses on opposite sides of a front.

Figs. 1c,d show the net abiotic response in surface pCO₂. Here, the effects of biological consumption are not included. Comparison with the panels above (showing the net effect with biological uptake) reveals that in most regions, biological uptake does not have a dominant role in modifying the pCO₂ response on these scales. This is with the exception of some high latitude regions in summer, but the results are not reliable in the Southern ocean, where NO₃ is known to remain unconsumed in the surface ocean. When estimating the biological contribution, no time lag is considered and the biological uptake is assumed to be NO₃ limited.

To estimate the absolute change in surface pCO₂ that would result from such perturbations, we multiply the relative change in pCO₂ by the monthly, climatological surface pCO₂ (Takahashi, et al., 2009). The resulting patterns in surface pCO₂ variation (Fig. 1e,f) are similar to the relative pCO₂ change (Fig. 1a,b), and show little or no similarity to the monthly pCO₂ distribution. This suggests that the pCO₂ response to vertical mixing is governed by the subsurface gradients in the various properties, and not by the value of the surface pCO₂ per se. The largest variations in surface pCO₂ occur in the eastern upwelling regions and western boundary currents, and are in the range of -75 – +60 μ atm for the chosen strength of mixing.

(b) *Effects of individual properties*

To tease apart the contribution of individual factors to the relative change in surface pCO₂, we plot each of the terms in (2.5). These are referred to as the TEM effect = $-\frac{\kappa\Delta t}{H}(\beta\frac{\partial T}{\partial z})$, DIC effect = $-\frac{\kappa\Delta t}{H}\left(\frac{\xi}{\text{DIC}}\frac{\partial \text{DIC}}{\partial z}\right)$, ALK effect = $-\frac{\kappa\Delta t}{H}\left(\frac{\xi_A}{\text{ALK}}\frac{\partial \text{ALK}}{\partial z}\right)$ and BIO effect = $-\frac{\kappa\Delta t}{H}R_{C:N}L\frac{\partial \text{NO}_3}{\partial z}$. The contributions of salinity and S_{ALK} are small and are not shown. Fig. 2 shows global maps of the remaining factors in January and July. The effect of DIC is opposite to that of T. While the entrainment of cooler water from subsurface lowers surface pCO₂ (indicated by blue shades in Fig. 2a,b) the consequent enhancement in surface DIC increases surface pCO₂, and is consequently shown in yellow and red colours (Fig. 2c,d). A vertical flux of ALK from the subsurface can either increase or decrease surface pCO₂ according to whether the vertical gradient in ALK is positive or negative (Fig. 2e,f). The vertical supply of NO₃ results in an uptake of DIC (lowering pCO₂ as indicated in blue; Fig. 2g,h), which offsets some of the DIC fluxed in to the ML. Grey regions indicate a lack of sensitivity of surface pCO₂ to upwelling. The examination of individual factors explains why one might see a large change in pCO₂ due to upwelling at certain locations, but not at others.

Amongst the various factors, DIC, T and BIO can make a maximum contribution of about 25% in certain regions, whereas ALK has a smaller range of approximately $\pm 10\%$. We would expect the BIO effect to be generally negative since NO₃ increases with depth and mixing causes an enhancement of NO₃ and consumption of DIC in the ML. But the use of an average value over the ML can sometimes cause an unphysical reversal of gradient at the base, giving rise to a weak positive BIO effect in some regions.

Fig. 2 indicates that the surface pCO₂ is most responsive to upwelling in the western boundary systems and coastal upwelling zones. South of the Gulf Stream and Kuroshio temperature has a controlling effect on pCO₂ variations, such that surface pCO₂ would be lowered in response to upwelling. North of the Gulf Stream

and Kuroshio, DIC has a dominant effect and $p\text{CO}_2$ would increase in response to upwelling. The upwelling region off the west coast of Central America also shows alternating positive and negative perturbations along the coast, with a dominance of the DIC effect off Chile, dominance of the BIO effect off the Peruvian upwelling zone, and DIC dominance further north toward Baja California.

Our results suggest that the response of surface $p\text{CO}_2$ to mixing varies regionally and temporally. Various effects can dominate the $p\text{CO}_2$ perturbation. Fig. 2i,j indicates which effect dominates in a given region during January and July. If the dominant effect does not control the surface $p\text{CO}_2$ variation (i.e. if the response is opposite in sign), we leave the region grey. Since the effects of ALK and salinity are relatively small, the surface $p\text{CO}_2$ is, in general, lowered by upwelling when the effect of T plus biology (BIO) exceeds the effect of upwelled DIC. In most regions of the ocean, the effect of DIC dominates, although BIO and TEM effects do exceed the DIC effect in certain regions. In regions where the temperature or NO_3 effect dominates, $p\text{CO}_2$ will be lowered due to vertical fluxes (assuming the alkalinity effect is negligible).

(c) Seasonally varying response at specific sites

To examine the processes responsible for the seasonal changes in $p\text{CO}_2$ due to localized mixing more closely, Figure 3 presents monthly results for four specific sites, namely the Joint Global Ocean Flux Study (JGOFS) sites of the Bermuda Atlantic Time-Series (BATS) and Hawaii Ocean Time-series (HOT), as well as the North Atlantic Bloom Experiment (NABE site at 47N) and the Antarctic Polar Frontal Zone (APFZ) site. In general, the largest potential changes in $p\text{CO}_2$ arising from localized mixing events occurs in the summer, when the mixed layer is shallowest and the gradients at its base are sharpest. In the wintertime, deep mixed layers result in a relatively homogenous water column and the impacts of mixing are thus minimized. Nevertheless, it is also important to note that the degree of density stratification is greatest during the summer, which may make it more difficult to obtain a large vertical flux.

If we first examine the subtropical stations BATS and HOT, we find that although the DIC effect consistently increases $p\text{CO}_2$ year round (Fig. 3), the impact of temperature is different between the two sites. The TEM effect contributes a large reduction in $p\text{CO}_2$ during the summertime at BATS, whereas it makes virtually no contribution at HOT. This is because the thermocline is much sharper and shallower at BATS relative to HOT (for example between 0 and 100m, Fig. 3), which leads to a greater cooling of surface waters and hence a reduction in $p\text{CO}_2$ in response to localized mixing. The impact of biological production at both sites is of little consequence, because the nitricline is consistently deeper than the mixed layer (i.e., the depth across which anomalous mixing occurs, Figure 3). Accordingly, at BATS, the TEM effect (and to a lesser extent the ALK effect) can more than offset the increased $p\text{CO}_2$ due to DIC in summer and mixing contributes to a net reduction in $p\text{CO}_2$ between May and August. At HOT, the TEM effect is too weak to counter-balance the DIC effect and mixing results in a small relative increase in $p\text{CO}_2$.

At the high latitude stations (NABE and APFZ) there is a great deal of seasonality. At NABE, mixing has little impact during the winter, since mixed layers

are already very deep ($>200\text{m}$). In the spring and summertime, mixing of DIC increases pCO_2 greatly and the counter-balancing effect of temperature is not as large as at BATS. Hence, the net effect of all abiotic processes results in a net increase in pCO_2 in response to localized mixing between March and November (Fig. 3). However, the biological effect during the spring to autumn period is much larger than at BATS or HOT, because the nitricline is much shallower, and is thus almost able to offset the net effect of abiotic processes for much of the spring and summer. Including the impact of biology means that mixing actually leads to a net reduction in pCO_2 during September and October (Figure 3). However, it is important to note that biology needs to act in concert with T to drive the reduction in pCO_2 during this period. The APFZ similarly shows large changes throughout the year. As seen previously, mixing of DIC causes large increases in pCO_2 even in the winter (as winter mixed layers are shallower than at NABE). This is offset slightly by the combination of the smaller effects of T and ALK during the spring and summer, but still results in a net increase in pCO_2 due to abiotic processes. Localised mixing causes a large net reduction in pCO_2 between November and March. This is due to a large increase in biological productivity associated with the increased vertical flux of NO_3 that can more than counter balance the net increase in pCO_2 associated with abiotic processes. However, the BIO effect might be over estimated in the iron limited APFZ if the ferricline were deeper than the nitricline. The biological response to a localized mixing event is based on the NO_3 profile and assumes a fixed C/N ratio. However, increasing the supply of iron to phytoplankton results in a concomitant increase in their demand for iron (Sunda & Huntsman, 1997; Dutreuil *et al.*, 2009). This would be translated into a reduction in the C/Fe ratio in response to an increased vertical flux of iron associated with a localized mixing event. As such, our results regarding the biological response should be seen as maximal effects in the iron limited Southern Ocean.

Overall, we find that there are often compensatory processes that act in concert to moderate or enhance the response of surface pCO_2 to localized mixing on a month by month basis. While DIC always drives an increase in surface pCO_2 , T and/or BIO are able to compensate for this effect during the summertime and cause a net reduction in pCO_2 at some stations. Biology is generally weak in the tropics and T can cause a seasonal reduction in pCO_2 at BATS, but not at HOT. This is due to variability in the thermocline depth, relative to the depth of mixing between each station. On the other hand, the TEM effect is weaker at high latitudes (NABE and APFZ) and biological activity is the predominant means by which the impact of DIC is offset to cause a net pCO_2 reduction in summer. The combination of T and BIO is more important at NABE than at APFZ, although we note that the BIO effect might be overestimated at APFZ.

5. Discussion

The proposed framework allows us to synthesize the findings of several recent studies that have examined the response of the surface ocean to upwelling or mixing events. Bates *et al.* (1998) found that in the Sargasso sea, the surface ocean cooled by several degrees with the passing of hurricane Felix in 1995. The lowered temperature affected the surface pCO_2 , which was lowered by $60 \mu\text{atm}$. A similar effect was reported by Koch *et al.* (2009). This is consistent with our analysis (Fig. 2, right

column) which shows that in the region of the Sargasso Sea, the effect of temperature (TEM effect) dominates the change in surface $p\text{CO}_2$ induced by mixing during summer. Further to the north (at 72.5W, 39.5N), the passage of extra-tropical hurricane Gustav (2002) caused no significant cooling, but an increase sea surface $p\text{CO}_2$ of $50\mu\text{atm}$ due to the enhancement of DIC (Perrie *et al.*, 2004). This too is consistent with Fig. 1 and Fig. 2, which show the dominance of the DIC effect and potential increase in $p\text{CO}_2$ due to mixing in this region over the summer.

Modeling studies that were based on conditions in the North Atlantic during the summer (Mahadevan *et al.*, 2004), as well as winter (Resplandy *et al.*, 2009), revealed that upwelling induced by fronts and eddies generates little or no change in the surface $p\text{CO}_2$. This is consistent with our results, since we find that the change in $p\text{CO}_2$ in the NE Atlantic is negligible in January (Fig. 1a) and less than $5\mu\text{atm}$ in July, largely because the effects of lowered T and increased DIC negate each other. The largest changes in the North Atlantic are actually found on the western side, north of the Gulf Stream in January and on either side of the Gulf Stream in July, due to stronger DIC gradients. However, it should be noted that impacts of submesoscale dynamics on surface $p\text{CO}_2$ do not only include vertical processes. Both modeling studies have indeed revealed very clearly that lateral stirring by mesoscale eddies of surface water masses with substantially different $p\text{CO}_2$ generates strong gradients in surface $p\text{CO}_2$, in agreement with those observed in the field (Watson *et al.*, 1991; Resplandy *et al.*, 2009). This effect, not considered here, mainly redistributes $p\text{CO}_2$ at small spatial scales without significantly modifying its mean value, which is not the case when vertical fluxes are involved.

There are some important implications for the response of surface $p\text{CO}_2$ to episodic vertical fluxes. Regions and times that show a large sensitivity of surface $p\text{CO}_2$ to vertical mixing can be expected to exhibit greater spatial and temporal variance in surface $p\text{CO}_2$, which has consequences for calculating carbon budgets (Monteiro *et al.*, 2009). Secondly, changes in $p\text{CO}_2$ are concomitant with a change in seawater pH, or ocean acidification. Thus, this analysis helps to identify regions that would be particularly vulnerable to changes in pH, such as the west coast of North America where marine ecosystems could be at stake (Feely *et al.*, 2008). On the other hand, we expect that the impact of mixing-induced perturbations in surface $p\text{CO}_2$ on large-scale air-sea CO_2 fluxes would be negligible due to the limited area and duration of the $p\text{CO}_2$ modulations (Lenton *et al.*, 2006). In some instances, however, as in the case of hurricanes, a systematic correlation with higher wind speeds and gas exchange rates could enhance the sea-to-air gas flux as reported by Bates *et al.* (1998).

Estimates of the BIO effect in this framework should be viewed with some caution. Our present results indicate that the effect of DIC broadly dominates the $p\text{CO}_2$ perturbation, and that vertically fluxed NO_3 does not account for the complete consumption (in Redfield proportion) of vertically fluxed DIC. In reality, the biological response to the vertical flux of nutrients is complex, depending on species composition, micro nutrients, variable stoichiometric ratios and variability in PAR. Thus it is often difficult to capture the biological response even with ecosystem models, and the simplistic approach taken here may very well underestimate the biological contribution. Furthermore, we point out the potential for inconsistencies amongst the data sets used in this study since they are constructed from varied sources of data with different methods.

474 In the future, with climate change, we would expect an increase in surface ocean
 475 temperatures and vertical gradients in temperature. Consequently, the negative
 476 perturbation of T on pCO₂ due to mixing (TEM effect) would be enhanced, even
 477 as surface pCO₂ is likely to be higher due to higher surface T and DIC. Increasing
 478 surface DIC due to the uptake of anthropogenic CO₂ will reduce the positive effect
 479 of DIC on surface pCO₂ in response to mixing. Using the GLODAP data, we can
 480 estimate that the vertical gradient in DIC (between the surface and depths of 100m–
 481 300m) has already declined by 5-10% since the pre-industrial. Thus, the net effect
 482 is likely to be a reduction in the dominance of the DIC effect and increase in the
 483 dominance of the TEM effect, tending to decrease the surface pCO₂ perturbation
 484 (or make it more negative) in response to mixing. However, the effects of subduction
 485 and circulation are known to complicate this simple picture by sequestering more
 486 anthropogenic CO₂ at depth than at the surface in some locations. It is also likely
 487 that climate change will modify the degree of stratification (Sarmiento *et al.*, 2004),
 488 which may impact the strength and frequency of episodic mixing events in the
 489 future.

490 6. Conclusions

491 We propose an analytical framework that we apply to observational datasets for
 492 analyzing the impact of vertical fluxes in DIC, ALK, T, S and NO₃ on sea surface
 493 pCO₂. We make a global, monthly, assessment of the surface pCO₂ perturbations
 494 due to episodic mixing of a given strength. We find a great deal of spatial and
 495 temporal variability in the pCO₂ response at the sea surface, with the amplitude
 496 of the perturbation exceeding 20 μatm in many regions, and being positive in some
 497 areas and negative in others. The largest surface pCO₂ response to vertical mixing
 498 is found in eastern upwelling margins and regions with shallow mixed layers during
 499 the summer. The response depends on the interactive effects of DIC, T, ALK and
 500 biology, which can compensate or reinforce their individual effects. This explains
 501 why a given mixing event (e.g., the passage of a hurricane or vertical advection from
 502 frontogenesis) can elicit an increase or a decrease in surface pCO₂ depending on
 503 its precise location and timing. In general, entrainment of DIC from the subsurface
 504 increases surface pCO₂, while a reduction in T and the biological uptake of DIC
 505 act to reduce pCO₂. The response due to ALK is spatially variable. In the future,
 506 climate change will likely modify the oceanic mean vertical gradients of temper-
 507 ature and DIC due to the uptake of anthropogenic CO₂, thereby reducing pCO₂
 508 perturbations and variability arising from vertical mixing, even as the mean surface
 509 pCO₂ may be higher.

510 **Acknowledgements:** A.M. acknowledges support from NASA grant NNX08AL80G, and
 511 A.L. from the Australian Climate Change Science Program.

512 References

- 513 Antonov, J., Locarnini, R., Boyer, T., Mishonov, A. & Garcia, H. 2006 World Ocean
 514 Atlas 2005, Volume 2: Salinity. Tech. rep., NOAA Atlas NESDIS 62, U.S. Government
 515 Printing Office, Washington, D.C., 182 pp.
- 516 Archer, D., Takahashi, T., Sutherland, S., Goddard, J., Chipman, D., Rodgers, K. &
 517 Ogura, H. 1996 Daily, seasonal and interannual variability of sea-surface carbon and

- 518 nutrient concentration in the equatorial Pacific Ocean. *Deep Sea Res. II Topical Studies*
519 *in Oceanogr.*, **43**(4-6), 779–808.
- 520 Bates, N., Knap, A. & Michaels, A. 1998 Contribution of hurricanes to local and global
521 estimates of air-sea exchange of CO_2 . *Nature*, **395**, 58–61. (doi:10.1038/25703)
- 522 Borges, A. & Frankignoulle, M. 2001 Short-term variations of the partial pressure of CO_2
523 in surface waters of the Galician upwelling system. *Prog. Oceanogr.*, **51**, 283–302.
- 524 Copin-Montégut, C., Bégovic, M. & Merlivat, L. 2004 Variability of the partial pressure of
525 CO_2 on diel to annual time scales in the northwestern Mediterranean Sea. *Mar. Chem.*,
526 **85**, 169–189.
- 527 de Boyer Montégut, C., Madec, G., Fischer, A., Lazar, A. & Iudicone, D. 2004 Mixed
528 layer depth over the global ocean: an examination of profile data and a profile-based
529 climatology. *J. Geophys. Res.*, **109**(C12003). (doi:10.1029/2004JC002378)
- 530 DeGrandpre, M., Hammar, T., Wallace, D. & Wirick, C. 1997 Simultaneous mooring-based
531 measurements of seawater CO_2 and O_2 off Cape Hatteras, North Carolina. *Limnol.*
532 *Oceanogr.*, **42**, 21–28.
- 533 Dutreuil, S., Bopp, L. & Tagliabue, A. 2009 Impact of enhanced vertical mixing on marine
534 biogeochemistry: Lessons for geo-engineering and natural variability. *Biogeosciences*, **6**,
535 901–912.
- 536 Feely et al., R. 2008 Evidence for upwelling of corrosive “acidified” water onto the conti-
537 nental shelf. *Science*, **320**(5882), 1490–1492. (doi:10.1126/science.1155676)
- 538 Garcia, H. E., Locarnini, R. A., Boyer, T. P. & Antonov, J. 2006 World Ocean Atlas 2005,
539 Volume 4: Nutrients (phosphate, nitrate, silicate). Tech. rep., NOAA Atlas NESDIS
540 64, U.S. Government Printing Office, Washington, D.C., 396 pp.
- 541 Hales, B., Takahashi, T. & Bandstra, L. 2005 Atmospheric CO_2 uptake by a coastal up-
542 welling system. *Global Biogeochem. Cycles*, **19**(GB1009). (doi:10.1029/2004GB002295)
- 543 Key, R., Kozyr, A., Sabine, C., Lee, K., Wanninkhof, R., Bullister, J., R.A. Feely, F. M.,
544 Mordy, C. & Peng, T.-H. 2004 A global ocean carbon climatology: Results from GLO-
545 DAP. *Global Biogeochem. Cycles*, **18**, GB4031.
- 546 Klein, P. & Coste, B. 1984 Effects of wind-stress variability on nutrient transport into the
547 mixed layer. *Deep Sea Res., A*, **31**, 21–37.
- 548 Klein, P., Hua, B. L., Lapeyre, G., Capet, X., Le Gentil, S. & Sasaki, H. 2008 Upper ocean
549 turbulence from high-resolution 3-D simulations. *J. Phys. Oceanogr.*, **38**, 1748–1763.
- 550 Koch, J., McKinley, G., Bennington, V. & Ullman, D. 2009 Do hurricanes cause signifi-
551 cant interannual variability in the air-sea CO_2 flux of the subtropical North Atlantic?
552 *Geophys. Res. Lett.*, **36**, L07606. (doi:10.1029/2009GL037553)
- 553 Körtzinger, A., Send, U., Lampitt, R., Hartman, S., Wallace, D., Karstensen, J., Villagar-
554 cia, M., Llinás, O. & DeGrandpre, M. 2008 The seasonal $p\text{CO}_2$ cycle at 49°N 16.5°W
555 in the northeastern Atlantic ocean and what it tells us about biological productivity.
556 *J. Geophys. Res.*, **113**(C04020). (doi:10.1029/2007JC004347)
- 557 Le Quééré, C., Raupach, M., Canadell, J. & et al., G. M. 2009 Trends in the sources and
558 sinks of carbon dioxide. *Nature Geoscience*, **2**, 831–836. (doi:10.1038/ngeo689)

- 559 Leinweber, A., Gruber, N., Frenzel, H., Friederich, G. & Chavez, F. 2009 Diurnal carbon
560 cycling in the surface ocean and lower atmosphere of Santa Monica Bay, California.
561 *Geophys. Res. Lett.*, **36**, L08 601. (doi:10.1029/2008GL037018)
- 562 Lengaigne, M., Madec, G., Bopp, L., Menkes, C., Aumont, O. & Cadule, P. 2009 Bio-
563 physical feedbacks in the Arctic Ocean using an earth system model. *Geophys. Res.*
564 *Lett.*, **36**(L21602). (doi:10.1029/2009GL040145)
- 565 Lenton, A., Matear, R. & Tilbrook, B. 2006 Design of an observational strategy for
566 quantifying the Southern Ocean uptake of CO₂. *Global Biogeochem. Cycles*, **20**. (doi:
567 10.1029/2005GB002620)
- 568 Lenton, A., Metzl, N., Takahashi, T., Sutherland, S., Tilbrook, B., Kuchinke, M. &
569 Sweeney, C. submitted The observed evolution of the trends and drivers of oceanic
570 pCO₂ over the last two decades. *Global Biogeochem. Cycles*.
- 571 Lévy, M., Klein, P. & Jelloul, M. B. 2009 New production stimulated by high-frequency
572 winds in a turbulent mesoscale eddy field. *Geophys. Res. Lett.*, **36**(16), L16 603.
- 573 Lévy, M., Klein, P. & Treguier, A. M. 2001 Impacts of sub-mesoscale physics on production
574 and subduction of phytoplankton in an oligotrophic regime. *J. Mar. Res.*, **59**, 535–565.
- 575 Locarnini, R., Mishonov, A., Antonov, J., Boyer, T. & Garcia, H. 2006 World Ocean Atlas
576 2005, Volume 1: Temperature. Tech. rep., NOAA Atlas NESDIS 61, U.S. Government
577 Printing Office, Washington, D.C., 182 pp.
- 578 Lovelock, J. & Rapley, C. G. 2007 Ocean pipes could help the earth to cure itself. *Nature*,
579 **447**, 403.
- 580 Mahadevan, A. & Archer, D. 2000 Modeling the impact of fronts and mesoscale circulation
581 on the nutrient supply and biogeochemistry of the upper ocean. *J. Geophys. Res.*,
582 **105**(C1), 1209–1225.
- 583 Mahadevan, A., Lévy, M. & Mémerly, L. 2004 Mesoscale variability of sea sur-
584 face pCO₂: What does it respond to? *Global Biogeochem. Cycles*, **18**(1),
585 GB101 710.10292003GB002 102.
- 586 McGillicuddy, Jr., D., Robinson, A., Siegel, D., Jannasch, H., Johnson, R., Dickey, T., Mc-
587 Neil, J., Michaels, A. & Knap, A. 1998 Influence of mesoscale eddies on new production
588 in the Sargasso Sea. *Nature*, **394**, 263–266.
- 589 Merlivat, L., Davila, M. G., Caniaux, G., Boutin, J. & Reverdin, G. 2009 Mesoscale and diel
590 to monthly variability of CO₂ and carbon fluxes at the ocean surface in the northeastern
591 Atlantic. *J. Geophys. Res.*, **114**(C3), C03 010. (doi:10.1029/2007JC004657)
- 592 Monteiro et al., P. 2009 A global sea surface carbon observing system: Assessment of
593 changing sea surface CO₂ and air-sea CO₂ fluxes. Tech. rep., OceanObs Community
594 White Paper, 1–25 September 2009, Venice, Italy.
- 595 Perrie, W., Zhang, W., Ren, X., Long, Z. & Hare, J. 2004 The role of midlatitude storms on
596 air-sea exchange of CO₂. *Geophys. Res. Lett.*, **31**, L09 306. (doi:10.1029/2003GL019212)
- 597 Pollard, R. & Regier, L. 1992 Vorticity and vertical circulation at an ocean front. *J. Phys.*
598 *Oceanogr.*, **22**, 609–625.

- 599 Resplandy, L., Lévy, M., dOvidio, F. & Merlivat, L. 2009 Impact of submesoscale
600 variability in estimating the air-sea CO_2 exchange: Results from a model study of
601 the POMME experiment. *Global Biogeochem. Cycles*, **23**(GB1017), 19pp. (doi:
602 10.1029/2008GB003239)
- 603 Sarmiento, J. & Gruber, N. 2006 *Ocean biogeochemical dynamics*. Princeton University
604 Press, Princeton, USA.
- 605 Sarmiento, J., Slater, R., Barber, R., Bopp, L., Doney, S., Hirst, A., Kleypas, J., Matear,
606 R., Mikolajewicz, U. *et al.* 2004 Response of ocean ecosystems to climate warming.
607 *Global Biogeochem. Cycles*, **18**(GB3003). (doi:10.1029/2003GB002134)
- 608 Sunda, W. & Huntsman, S. 1997 Interrelated influence of iron, light and cell size on marine
609 phytoplankton growth. *Nature*, **390**, 389–392.
- 610 Takahashi, T., Olafsson, J., Goddard, J., Chipman, D. & Sutherland, S. C. 1993 Seasonal
611 variation of CO_2 and nutrients in the high-latitude surface oceans: A comparative study.
612 *Global Biogeochem. Cycles*, **7**(4), 843–878.
- 613 Takahashi, et al. 2009 Climatological mean and decadal change in surface ocean $p\text{CO}_2$,
614 and net sea-air CO_2 ux over the global oceans. *Deep Sea Res. II*, **56**, 554577. (doi:
615 10.1029/2004JC002378)
- 616 Walsh, J. 1978 A data set on northern hemisphere sea ice extent, 1953-1976. Tech. Rep.
617 Report GD-2, 49-51, World Data Center for Glaciology (Snow and Ice).
- 618 Wanninkhof, R. 1992 Relationship between wind speed and gas exchange over the ocean.
619 *J. Geophys. Res.*, **97**(C5), 7373–7382.
- 620 Watson, A., Robinson, C., Robinson, J., B.Williams, P. L. & Fasham, M. 1991 Spatial
621 variability in the sink for atmospheric carbon dioxide in the North Atlantic. *Nature*,
622 **350**, 50–53.
- 623 Yool, A., Shepherd, J., Bryden, H. & Oschlies, A. 2009 Low efficiency of nutrient translo-
624 cation for enhancing oceanic uptake of carbon dioxide. *J. Geophys. Res.*, **114**(C08009).
625 (doi:10.1029/2008JC004792)
- 626 Zwally, H., Comiso, J., Parkinson, C., Campbell, W., Carsey, F. & Gloerson, P. 1983
627 Antarctic sea ice, 1973-1976: Satellite passive microwave observations. Tech. rep.,
628 NASA.

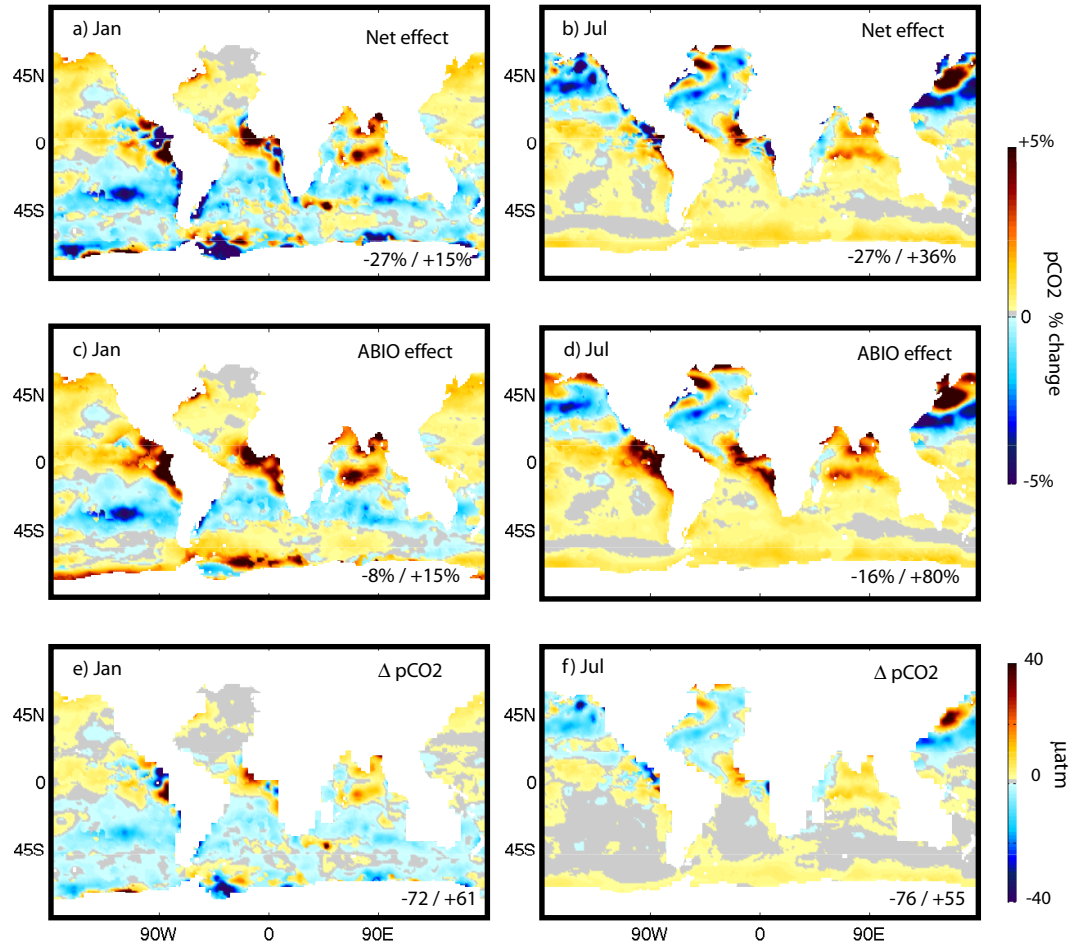


Figure 1. Left and right columns contrast results for January and July. Panels a and b show the net relative change in surface pCO₂, due the sum of various effects in January and July, respectively. Panels c and d show the relative change in pCO₂ due to abiotic effects, i.e. without taking into account BIO, the uptake of DIC by phytoplankton production supported by a NO₃ flux. Panels e and f show the net change in pCO₂ (resulting from all effects) in response to vertical mixing, based on the climatological monthly pCO₂ (Takahashi, et al., 2009). The ABIO (abiotic) effect is the sum of TEM, DIC, ALK and S effects, whereas the net effect comprises the ABIO and BIO effects.

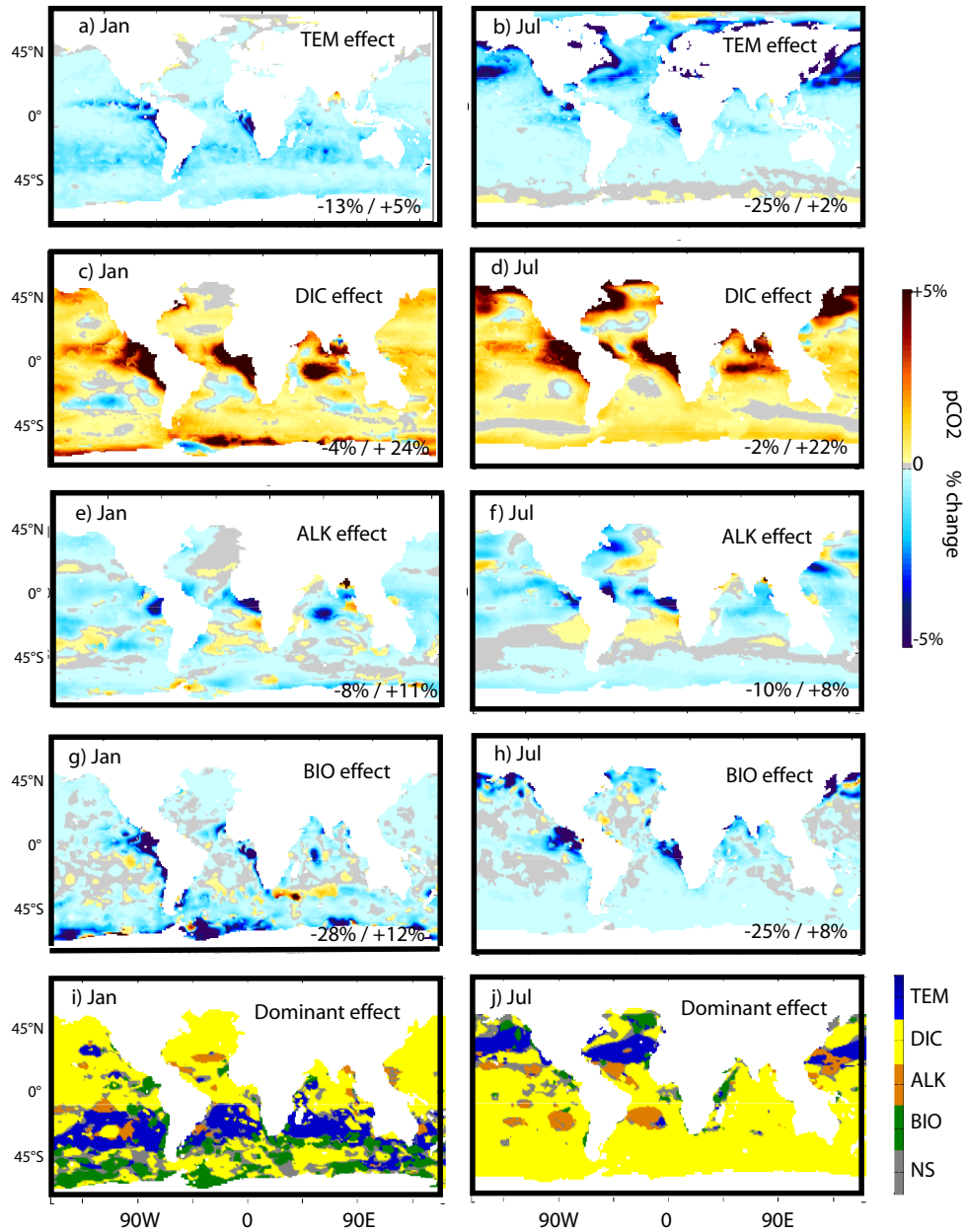


Figure 2. Percent change in surface $p\text{CO}_2$ in response to localized vertical mixing separated into various factors: (a-b) TEM, (c-d) DIC, (e-f) ALK, (g-h) BIO, i.e. biological uptake due to inputs of NO_3 . For panels a to h the range of results is presented in the lower right section of each panel. The lowermost panels, (i-j), indicate which of these factors has the largest influence on surface $p\text{CO}_2$; 'NS' indicates the factor is not significant because it is overrun by opposing influences. These effects are estimated for January (left column) and July (right column). TEM and BIO would lower surface $p\text{CO}_2$, whereas DIC would enhance surface $p\text{CO}_2$. ALK may have either sign. Each of the effects becomes stronger in regions experiencing summer. These estimates are for a vertical diffusivity of $10^{-3} \text{m}^2 \text{s}^{-1}$ acting at the base of the mixed layer for a day, but stronger/weaker mixing would result in a proportionally higher/lower perturbation in $p\text{CO}_2$.

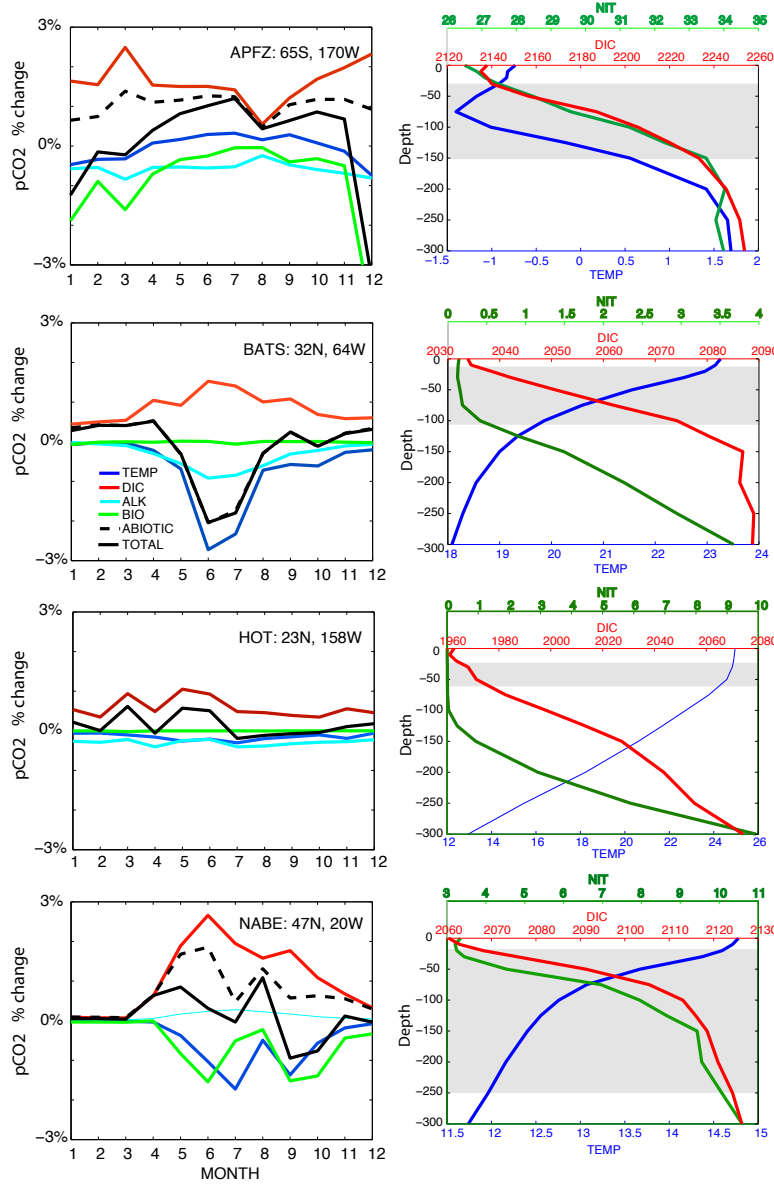


Figure 3. The results are contrasted amongst various oceanic regions through time-series and profiles averaged over a $5^\circ \times 5^\circ$ region centered on the Antarctic Polar Frontal Zone (APFZ at 65S, 170W), Bermuda Atlantic Time Series (BATS at 32N, 64W), Hawaii Ocean Time series (HOT at 23N, 158W) and the site of the North Atlantic Bloom Experiment (NABE at 47N, 20W). Left column: Annual monthly time series showing the relative change in surface $p\text{CO}_2$ arising from the upwelling/mixing related effects of TEM, DIC, ALK, BIO, the total abiotic component ABIO, and the net sum of all effects. Positive/negative values indicate the potential for a relative increase/decrease in surface $p\text{CO}_2$, due to mixing represented by $\kappa = 10^{-3} \text{ m-s}^{-2}$ acting at the base of the mixed layer for one day. Right column: Annual mean vertical profiles of temperature (deg. C), DIC ($\mu\text{mol/l}$) and NO_3 ($\mu\text{mol/l}$) at the same sites from climatological data. The range in MLD over the annual cycle is shaded grey.